Radiocarbon, Vol 61, Nr 1, 2019, p 195–210 DOI:10.1017/RDC.2018.81


# MARINE RADIOCARBON RESERVOIR AGE ALONG THE CHILEAN CONTINENTAL MARGIN

Víctor Merino-Campos[1] • Ricardo De Pol-Holz[2*] • John Southon[3] • Claudio Latorre[4] • Silvana Collado-Fabbri[1]

[1]Postgraduate School in Oceanography, Faculty of Natural and Oceanographic Sciences, Universidad de Concepción, Chile.
[2]Dirección Programas Antárticos y Subantárticos and Center for Climate and Resilience Research (CR)[2], Universidad de Magallanes, Punta Arenas, Chile.
[3]Department of Earth System Science, University of California, Irvine, USA.
[4]Department of Ecology, Pontificia Universidad Católica de Chile, Santiago, Chile.

**ABSTRACT.** We present 37 new radiocarbon ($^{14}$C) measurements from mollusk shells fragments sampled along the Chilean continental margin and stored in museum collections with known calendar age. These measurements were used to estimate the modern pre-bomb regional marine $^{14}$C age deviations from the global ocean reservoir ($\Delta$R). Together with previously published data, we calculated regional mean $\Delta$R values for five oceanographic macro regions along the coast plus one for a mid-latitude open ocean setting. In general, upwelling regions north of 42ºS show consistent although sometimes highly variable $\Delta$R values with regional averages ranging from 141 to 196 $^{14}$C yr, whereas the mid-latitude open ocean location of the Juan Fernández archipelago and the southern Patagonian region show minor, $\Delta$R of $40 \pm 38$ $^{14}$C yr, and $52 \pm 47$ $^{14}$C yr respectively. We attribute the alongshore decreasing pattern toward higher latitudes to the main oceanographic features along the Chilean coast such as perennial coastal upwelling in northern zone, seasonally variable upwelling at the central part and the large freshwater influence upon the southern Patagonian channels.

**KEYWORDS:** Chile, radiocarbon AMS dating, reservoir correction, reservoir effect, upwelling.

## INTRODUCTION

The calibration of radiocarbon ($^{14}$C) ages of terrestrial materials requires a good record of the well-mixed atmospheric$^{14}$C concentration for the last 50,000 yr. This record has been built based on tree-ring, varved lake sediments, and speleothem data (Reimer et al. 2013). For marine samples, however, a record of past surface ocean $^{14}$C activity is available derived from planktonic foraminifera and warm water corals, showing a mean difference of ~400 $^{14}$C yr from that of the atmosphere (Hughen et al. 2004). This difference is known as the marine reservoir age or "R" (Stuiver et al. 1986; Stuiver and Braziunas 1993) and it is the result of the mixing of the surface ocean with older, deeper waters (Broecker 1987; Broecker et al. 1991; Stuiver and Braziunas 1993). A critical complication arises since the rate of mixing can be very different in different parts of the ocean, leading to spatial differences in the value of R, like those found in high latitudes (Heier-Nielsen et al. 1995; Berkman and Forman 1996) or zones with strong upwelling regimes like the southeast Pacific (Southon et al. 1995). It is therefore mandatory to have an accurate (as much as possible) knowledge of the regional $^{14}$C age difference from that of the global mean or what is called $\Delta$R (Stuiver and Braziunas 1986; for a complete recent review see Alves et al. 2018). This value can be positive (older age than global surface ocean waters) like in upwelling regions, or negative (younger) like in highly stratified systems (Ascough et al. 2005; Hinojosa et al. 2015). There have been considerable efforts in trying to assess $\Delta$R values associated to different oceanic regimes, given their importance in paleoceanographic reconstructions and age model accuracy. For example, in the Gulf of California, Goodfriend and Flessa (1997) calculated a $\Delta$R of $550 \pm 108$ and $408 \pm 122$ $^{14}$C yr for the northern and central gulf samples (all cited values were updated using the latest marine calibration curve [Reimer et al. 2013]), respectively. This high reservoir age corresponds to a region with strong upwelling of deeper waters. Culleton et al. (2006) studied intra-shell marine reservoir corrections

*Corresponding author. Email: ricardo.depol@umag.cl.

from the Santa Barbara Channel region, and found modern ΔR mean values of 366 ± 35 and 278 ± 45 $^{14}$C yr, with ranges of 180 and 240 $^{14}$C yr respectively. This variability was also associated with the presence of coastal upwelling of deeper waters, together with seasonal inputs of $^{14}$C derived from terrestrial runoff. Southon et al. (2002) presented ΔR data for other upwelling zones such as the Arabian Sea, with mean regional values ranging from 154 ± 25 to 213 ± 30 $^{14}$C yr, and for the South China Sea, with values close to zero due to the presence of Pacific waters with high $^{14}$C content. Petchey et al. (2008) presented 31 reservoir correction ages for an open-ocean zone as the South Pacific subtropical gyre, with most of the values near zero due to the stable surface water conditions imposed by the ocean circulation. On the other hand, Hinojosa et al. (2015) investigated $^{14}$C reservoir ages in the fjord zone of southwest New Zealand, obtaining a ΔR of 59 ± 35 $^{14}$C yr. This value was related to the influence of $^{14}$C-depleted subantarctic water into the fjords, which may lead to greater reservoir ages in the region. In a similar context, Heier-Nielsen et al. (1995) found low reservoir ages for the Danish coastal zone with a mean ΔR value of 29 ± 16 $^{14}$C yr, derived from the North Atlantic and the North Sea.

Precise knowledge of ΔR is of particular importance for regions with large oceanographic and hydrographic contrasts like the coast of Chile. Located at the western south margin of the South American continent from ~18°S to ~56°S, it is characterized by (1) different upwelling-regime zones (permanent to seasonal) from the north (~18°S) to central-south (~40°S) Chile (Letelier et al. 2009); (2) increasing input of freshwater through precipitation and continental runoff toward the south (Torres et al. 2011); (3) the presence of fjords and glaciers that are remnants of the last Ice Age; and (4) the influence of Subantarctic waters (SAW) flowing northward associated to the Humboldt Current System (HCS) from around 44°S (Silva et al. 2009). The consequent latitudinal variations of $^{14}CO_2$ exchange between the atmosphere and the ocean caused by these factors, surely affects the $^{14}$C concentration (and subsequent age) of the surface waters along the Chilean coast.

Previous studies of ΔR along the Chilean coast have been carried out by Southon et al. (1995) from archeological sites in northern Chile (19ºS). They compared $^{14}$C ages of materials of terrestrial and marine origin, obtaining a ΔR range of 135 ± 110 $^{14}$C yr for the period 100–340 AD, up to 245 ± 85 $^{14}$C yr for the period 340–530 AD. Similarly, pre-bomb 20th century shell measurements of *Concholepas concholepas* at 24°S and *Tegula atra* at 33°S show a ΔR of 175 ± 41 and 315 ± 79 $^{14}$C yr, respectively (Taylor and Berger 1967). In contrast, Ingram and Southon (1996) reported pre-bomb mytilid shells from Valparaíso (33°S) with a lower ΔR of 60 ± 55 $^{14}$C yr. and for the inner Patagonian fjord of Puerto Natales (51°S) a relatively large ΔR of 220 ± 46 $^{14}$C yr. By studying Holocene variations of ΔR, Ortlieb et al. (2011) obtained a range of modern pre-bomb ΔR values for the northern Chilean coast between 20–23°S with a mean of 253 ± 207 $^{14}$C yr, showing high variability in ΔR associated to changes in upwelling regimes and/or by climatic oscillations like the ENSO cycle. Finally, Carré et al. (2016) and more recently Latorre et al. (2017) have calculated ΔR based on paired terrestrial-marine $^{14}$C measurements from Holocene shell middens in central and northern Chile, and show that, despite recent relatively stable oceanographic conditions, ΔR in this area can be highly variable at millennial time-scales.

Here we provide new modern pre-bomb estimates of ΔR for the Chilean Continental Margin based on $^{14}$C measurements on marine shells from museum collections of known age. In particular, our data fills a large gap in the regional knowledge of ΔR along the eastern South Pacific Ocean, where no ΔR information exists between 33º and 51ºS.

https://doi.org/10.1017/RDC.2018.81 Published online by Cambridge University Press

## REGIONAL SETTING

The general oceanographic setting of the eastern South Pacific is influenced by the Humboldt Current System (Figure 1). The northward Chile-Peru branch originates at about 45°S where the northern Circumpolar Current impinges against South America bifurcating into a northern component (Chile-Peru current) and a southern one (Cape Horn Current) (Silva and Neshyba 1977; Strub et al. 1998). The Chile-Peru current advects (SAW) at the surface, a water-mass characterized by very low values of salinity (<34.5) and temperature (<15ºC). SAAW also enters the south Chilean fjords area where it mixes with continental waters (Silva and Vargas 2014) while it is transported southward by the Cape Horn Current. The mixing causes further freshening due to the large freshwater input from Patagonian glaciers (Silva et al. 1997). The southward components of the Humboldt Current System, the Peru-Chile Countercurrent, transports Subtropical Surface Waters (SSW), while the Peru-Chile Undercurrent carries the Equatorial Subsurface Water (ESSW at the subsurface from about 10°S to 48°S (Silva and Neshyba 1979; Toggweiler et al. 1991). This water mass is characterized by high nutrient and low oxygen content and it is implicated in the upwelling process occurring along the coast. At the north, upwelling is a perennial feature while south of 30°S it is a highly seasonal process (Letelier et al. 2009).

South of 42°S, ice stream remnants of the last Ice Age (ca. 20,000 BP) supply large quantities of fresh-water and promote low salinity and cold temperatures along the coast (Acha et al. 2004), while wind speed increases southward reaching a maximum of 20 $ms^{-1}$ at the Polar Jet latitude band of near 40–50ºS (Torres et al. 2011). This has the important effect of increasing $CO_2$ solubility at the atmosphere-ocean interface (Wanninkhof and McGillis 1999). In addition, our southern study region (south of 40°S) is a highly productive environment due to the input of continentally derived nutrients (like iron and silica) from freshwater runoff along the Patagonian Fjords, which contributes further to regionally $CO_2$-undersaturated surface waters (Torres et al. 2011).

Torres et al. (2011) described $CO_2$ fluxes along the Chilean coast from 23°S to 56°S, comprising almost its entire latitudinal range. They found a strong relationship between $CO_2$ outgassing and the upwelling-regime zones as far south as ~40°S because of the presence of $CO_2$ supersaturated deeper waters at the surface, enhanced by heating at shallow depths. From ~42°S southward, cold coastal waters act as sink for $CO_2$ by the stratification of the water due to the great input of cold freshwater (Dávila et al. 2002) and increased rates of photosynthesis that result respectively in high $CO_2$ solubility and low $pCO_2$ at these latitudes.

## MATERIALS AND METHODS

Samples used in this study were provided by The Museum of Zoology of the University of Concepción (n = 11), and the collection of the Laboratory of Malacology at the National Museum of Natural History in Santiago, Chile (n = 26). We selected samples with labeled collection dates ranging between AD 1852 and 1960. Mollusks used in this work include gastropods and bivalves (Table 1). Bivalves selected were as follows: *Arca* sp., *Diplodonta inconspicua, Ensis macha, Gary solida, Glycimerys ovatus, Perumytilus purpuratus, Petricola rugosa, Tagelus dombeii, Ostrea chilensis.* Gastropods: *Crepidula sp., Fisurella cumingi, Littorina peruviana, Nacella clypeater, Nacella deaurata, Nacella magellanica, Nacella Polaris*, *Purpura xanthostoma, Scurria lacerata,* and *Scurria zebrina*. The available museum documentation that was present with the samples included: species name, sampling date and location of collection or broad geographical provenance (e.g. "Magallanes Region"). Our selected samples cover a

https://doi.org/10.1017/RDC.2018.81 Published online by Cambridge University Press

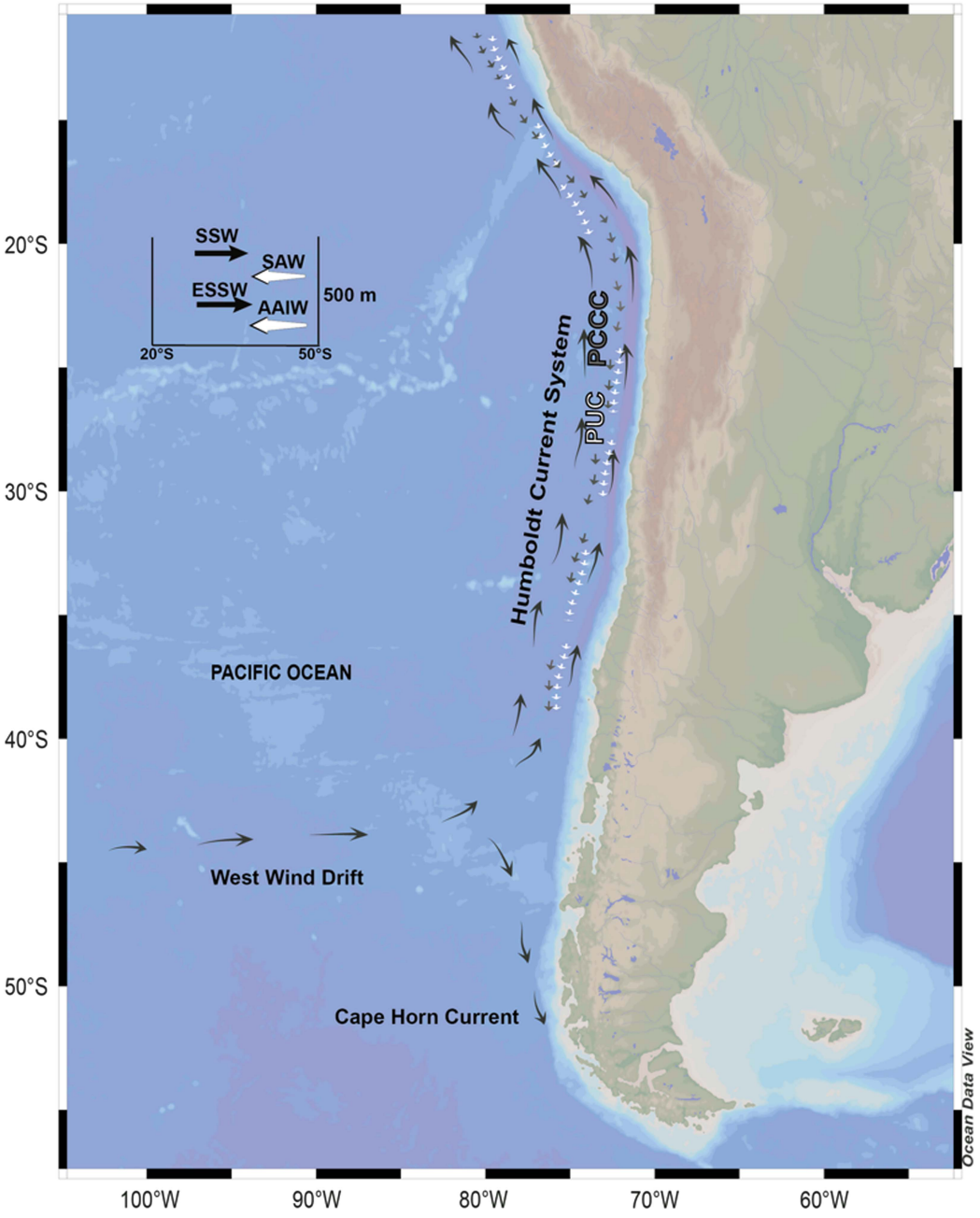


Figure 1 Surface ocean currents in the eastern South Pacific along the Chilean coast. The West Wind Drift feeds major currents flowing north/southward. Northward: the Humboldt Current and southward, the Cape Horn Current. The Perú-Chile Counter Current (PCCC) with its Undercurrent homologue (PCU). Subsurface and intermediate water masses are also shown (white: northward, black: southward). SSW: Sub Tropical Surface Water; SAW: Subantarctic Surface Water; EESW: Equatorial Subsurface Water; AAIW: Antarctic Intermediate Water.

https://doi.org/10.1017/RDC.2018.81 Published online by Cambridge University Press

Table 1 Modern reservoir age deviations along the Chilean coast (19º–55ºS).

| Lab code | Sample name | Location | $\delta^{13}C$ (‰ PDB)[a] | Date of collection (AD) | $^{14}C$ age (yr BP) | Marine13 Age (yr) | ΔR (yr) |
|---|---|---|---|---|---|---|---|
| **UCIAMS-144988#** | ***Glycimerys ovatus*** | **Arica (18°S)** | | **1948** | **48800 ± 1500** | | |
| Pa 2268* | *Protothaca thaca* | Salitrera Slavonia (20°S) | n.a. | 1900–1918 | 835 ± 40 | 451 ± 23 | 384 ± 46 |
| Pa 2250* | *Protothaca thaca* | Salitrera Buenaventura (21°S) | 1.2 | 1894–1930 | 645 ± 33 | 456 ± 23 | 189 ± 40 |
| C00-425a* | *Argopecten purpuratus* | Salitrera Prat (23°S) | 1.6 | 1912–1931 | 540 ± 60 | 451 ± 23 | 89 ± 64 |
| C00-425b* | *Argopecten purpuratus* | Salitrera Prat (23°S) | 1.7 | 1912–1931 | 795 ± 30 | 451 ± 23 | 344 ± 38 |
| C00-425c* | *Argopecten purpuratus* | Salitrera Prat (23°S) | 1.2 | 1912–1931 | 474 ± 32 | 451 ± 23 | 23 ± 39 |
| C00-425d* | *Argopecten purpuratus* | Salitrera Prat (23°S) | 1.1 | 1912–1931 | 598 ± 29 | 451 ± 23 | 147 ± 37 |
| UCLA1277** | *Concholepas concholepas* | Antofagasta (23°S) | 0.1 | 1925 | 626 ± 34 | 451 ± 23 | 175 ± 41 |
| | | | | | | **Weighed mean** | **196 ± 128** |
| UCIAMS-144986 | *Arca sp.* | Juan Fernández (33°S) | 2.32 | 1907 | 490 ± 30 | 449 ± 23 | 40 ± 38 |
| UCIAMS-142533*** | *Mesodesma donacium* | Coquimbo (30°S) | n.a. | 1837 | 605 ± 25 | 491 ± 23 | 146 ± 34 |
| UCLA-1278** | *Tegula atra* | Valparaíso (33°S) | 1.3 | 1930–1940 | 770 ± 76 | 454 ± 23 | 315 ± 79 |
| CAMS-17919**** | *Mytilus* sp. | Valparaíso (33°S) | 1.98 | 1939 | 520 ± 50 | 460 ± 23 | 60 ± 55 |
| UCIAMS-144995 | *Scurria zebrina* | Bucalemu (33°S) | 1.95 | 1954 | 550 ± 30 | 469 ± 23 | 80 ± 38 |
| UCIAMS-144993 | *Perumytilus purpuratus* | Valparaíso (33°S) | n.a. | 1956 | 580 ± 25 | 469 ± 23 | 110 ± 34 |
| UCIAMS-134080 | *Fisurella cumingi* | Valparaíso (33°S) | 1.17 | 1953 | 580 ± 20 | 469 ± 23 | 110 ± 30 |
| UCIAMS-134081 | *Scurria lacerata* | Valparaíso (33°S) | **n.a.** | 1953 | 730 ± 20 | 469 ± 23 | 260 ± 30 |
| **UCIAMS-134082#** | ***Littorina peruviana*** | **Valparaíso (33°S)** | **2.11** | **1953** | **450 ± 20** | | |
| | | | | | | **Weighed mean** | **148 ± 78** |
| UCIAMS-144972 | *Ensis macha* | Penco (37°S) | 0.55 | 1893 | 675 ± 25 | 459 ± 23 | 215 ± 34 |
| UCIAMS-144973 | *Ensis macha* | Penco (37°S) | 1.19 | 1893 | 625 ± 30 | 459 ± 23 | 165 ± 38 |

Table 1 (*Continued*)

| Lab code | Sample name | Location | $\delta^{13}C$ (‰ PDB)[a] | Date of collection (AD) | $^{14}C$ age (yr BP) | Marine13 Age (yr) | ΔR (yr) |
|---|---|---|---|---|---|---|---|
| UCIAMS-144979 | *Gary solida* | Sn. Vicente (37°S) | 2.21 | 1893 | 645 ± 30 | 459 ± 23 | 185 ± 38 |
| UCIAMS-144989 | *Diplodonta inconspicua* | Quiriquina Island (37°S) | n.a. | 1948 | 690 ± 25 | 469 ± 23 | 220 ± 34 |
| UCIAMS-144990 | *Diplodonta inconspicua* | Quiriquina Island (37°S) | 1.04 | 1948 | 675 ± 30 | 469 ± 23 | 205 ± 38 |
| UCIAMS-144991 | *Purpura xanthostoma* | Quiriquina Island (37°S) | 2.27 | 1948 | 640 ± 25 | 469 ± 23 | 170 ± 34 |
| | | | | | | **Weighed mean** | **194 ± 24** |
| **UCIAMS-144985[#]** | ***Glycimerys ovatus*** | **Niebla (39°S)** | **n.a.** | **1911** | **3830 ± 30** | | |
| **UCIAMS-144987[#]** | ***Glycimerys ovatus*** | **Niebla (39°S)** | **2.78** | **1960** | **6510 ± 30** | | |
| UCIAMS-144974 | *Ensis macha* | Pto. Montt (41°S) | –0.46 | 1911 | 665 ± 30 | 448 ± 23 | 215 ± 38 |
| UCIAMS-144976 | *Tagelus dombeii* | Pto. Montt (41°S) | 1.36 | 1911 | 565 ± 30 | 448 ± 23 | 115 ± 38 |
| UCIAMS-144971 | *Ensis macha* | Ancud (42°S) | 0.21 | 1953 | 605 ± 30 | 469 ± 23 | 135 ± 38 |
| UCIAMS-144975 | *Tagelus dombeii* | Ancud (42°S) | 2.06 | 1953 | 525 ± 25 | 469 ± 23 | 55 ± 38 |
| UCIAMS-144977 | *Tagelus dombeii* | Dalcahue (42°S) | 1.55 | 1959 | 535 ± 30 | 469 ± 23 | 65 ± 38 |
| UCIAMS-144978 | *Gary solida* | Ancud (42°S) | n.a. | 1951 | 570 ± 30 | 469 ± 23 | 100 ± 38 |
| UCIAMS-144980 | *Ostrea chilensis* | Ancud (42°S) | 1.68 | 1959 | 550 ± 25 | 469 ± 23 | 80 ± 34 |
| UCIAMS-144981 | *Ostrea chilensis* | Ancud (42°S) | 2.79 | 1952 | 605 ± 25 | 469 ± 23 | 135 ± 34 |
| UCIAMS-144983 | *Ostrea chilensis* | Ancud (42°S) | n.a. | 1880 | 650 ± 25 | 473 ± 23 | 175 ± 34 |
| UCIAMS-144994 | *Perumytilus purpuratus* | Pudeto River mouth (42°S) | 2.36 | 1951 | 585 ± 25 | 469 ± 23 | 115 ± 34 |
| UCIAMS-144996 | *Crepidula sp.* | Ancud (42°S) | n.a. | 1951 | 640 ± 25 | 469 ± 23 | 170 ± 34 |
| UCIAMS-144992 | *Purpura xanthostoma* | Castro (43°S) | 2.01 | 1894 | 640 ± 25 | 460 ± 23 | 180 ± 34 |
| UCIAMS-144982 | *Ostrea chilensis* | Asasao (43°S) | 0.43 | 1852 | 625 ± 25 | 485 ± 23 | 140 ± 34 |
| | | | | | | **Weighed mean** | **141 ± 43** |
| CAMS-17918**** | *Mytilus* sp. | Puerto Natales (51°S) | –2.32 | 1939 | 680 ± 40 | 460 ± 23 | 220 ± 46 |
| UCIAMS-144984 | *P.rugosa* | Strait of Magallanes (53°S) | –1.35 | 1955 | 510 ± 25 | 469 ± 23 | 40 ± 34 |

| | | | | | | | |
|---|---|---|---|---|---|---|---|
| UCIAMS-134083 | *Nacella magellanica* | Punta Chilota (53°S) | n.a. | 1953 | 495 ± 20 | 469 ± 23 | 25 ± 30 |
| UCIAMS-134084 | *Fisurella cumingi* | Bulnes Fort, Magallanes (53°S) | n.a. | 1954 | 505 ± 20 | 469 ± 23 | 35 ± 30 |
| UCIAMS-134085 | *Nacella clypeater* | Magallanes Region (53°S) | n.a. | 1954 | 505 ± 20 | 469 ± 23 | 35 ± 30 |
| UCIAMS-134086 | *Scurria zebrina* | Bulnes Fort, Magallanes (53°S) | 2.08 | 1954 | 505 ± 20 | 469 ± 23 | 35 ± 30 |
| UCIAMS-134090 | *Fisurella cumingi* | Punta Arenas (53°S) | 1.15 | 1956 | 475 ± 20 | 469 ± 23 | 5 ± 30 |
| UCIAMS-134087 | *Nacella deaurata* | Seno Almirantazgo (54°S) | n.a. | 1955 | 530 ± 20 | 469 ± 23 | 60 ± 30 |
| UCIAMS-134088 | *Nacella magellanica* | Seno Agostini (54°S) | 1.93 | 1954 | 530 ± 20 | 469 ± 23 | 60 ± 30 |
| **UCIAMS-134089[#]** | ***Nacella polaris*** | **Hoste Island (55°S)** | **n.a.** | **1954** | **–650 ± 20** | | |
| | | | | | | **Weighed mean** | **52 ± 47** |

*Ortlieb et al. (2011), **Taylor and Berger (1967), ***Carré et al. (2016), ****Ingram and Southon (1996).
[#]These samples were excluded from the calculation of the regional mean.
[a]$\delta^{13}C$ values of this study were measured at the stable isotope facility of the University of California at Davis.

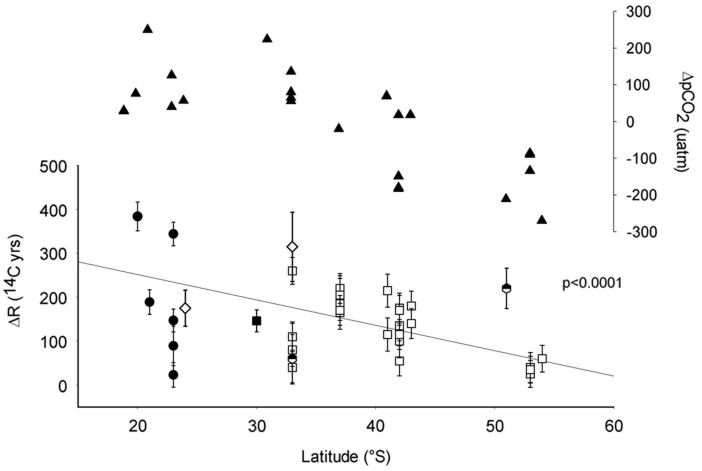


Figure 2 $\Delta pCO_2$ (difference in partial pressure of $CO_2$ between the ocean with respect to the atmosphere, upper panel) and all modern $\Delta R$ values existing for the Chilean coast (lower panel). A clear decreasing pattern can be observed in $CO_2$-saturation values from north to the south, similar to decreasing $\Delta R$ values. $\Delta pCO_2$ data extracted from Torres et al. (2011). In solid diamonds Taylor and Berger (1967), semi-filled hexagons Ingram and Southon (1996), filled circles Ortlieb et al. (2011) and black square Carré et al. (2016).

geographical span from Arica in northern Chile (19°S) to Hoste Island at the southern tip of South America (55°S).

For each selected individual, we used a Dremel® rotary tool for cutting 20–30 mg fragments from either the ventral side of bivalves, or from the outer lip of gastropod shells. These fragments were then leached to 50% of their weight using hydrochloric acid (0.1N) in order to remove any potential secondary carbonate and rinsed with deionized water. Samples were then hydrolyzed with 0.8 mL of 85% phosphoric acid by injecting acid through the septum of an evacuated vacutainer for ca. 30–60 min at 70°C. The $CO_2$ obtained from the samples was graphitized to 550°C by hydrogen reduction with an iron catalyst (Vogel et al. 1984; Loyd et al. 1991). $^{14}C$ measurements were performed at the W.M. Keck Carbon Cycle AMS Laboratory of the University of California, Irvine and $^{14}C$ ages were reported following the conventions of Stuiver and Polach (1977). $\Delta R$ values were calculated by subtracting the sample's conventional $^{14}C$ age from the Marine13 (Reimer et al. 2013) $^{14}C$ age at the calendar year labeled for each individual (see Southon et al. 1995 for a graphical description). For samples with calendar age later than 1950 AD we used the 1950 value of Marine13 as the model age. Individual $\Delta R$ errors where calculated as the square root of the sum of the analytical 1-sigma error and the model error squared. We also provide regional error-weighed mean $\Delta R$ values for 5 macro zones along the Chilean coast and their associated standard deviation.

In order to maximize our sample availability, we included many individuals collected between 1950 and 1960 AD. We recognize that this might not be ideal since some bomb-derived $^{14}C$ might be already present in the surface ocean (Ascough et al. 2005). This effect however should be very minor for the eastern South Pacific (see for example figure 4 in Druffel [1981]; figure 1 in Druffel and Griffin [1995] and figure 3 in Guilderson et al. [2000]) and we therefore chose to

https://doi.org/10.1017/RDC.2018.81 Published online by Cambridge University Press

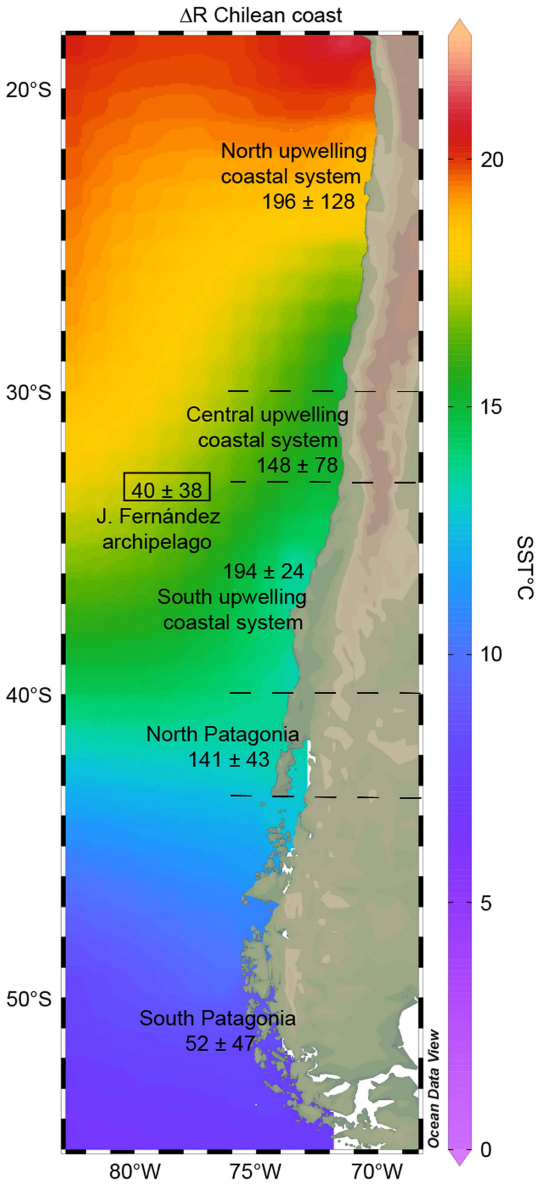


Figure 3 Mean regional ΔR values for the Chilean coast including previous studies. There are 5 regional values for the coast (gray) and one for the open ocean. Colors represent annual mean sea surface temperature obtained from the World Ocean Circulation Experiment (http://www.ewoce.org/). (Please see online version for color figures.)

include results of technically post-bomb shells. As mentioned before, for consistency previously published ΔR values were recalculated using the Marine13 calibration curve.

https://doi.org/10.1017/RDC.2018.81 Published online by Cambridge University Press

## RESULTS AND DISCUSSION

### $^{14}$C Ages

Table 1 shows the conventional $^{14}$C ages, collection date, location, and latitude for the 37 samples analyzed and data from previous studies in the region using known-age mollusk shells. Weighed mean ΔR values were calculated by proximity of location of the samples to establish a reliable and representative reservoir offset correction. All existing ΔR for the Chilean coast as a function of latitude are shown in Figure 2. Apparent $^{14}$C ages range from –650 ± 20 to 48,800 ± 1500 $^{14}$C yr and ΔR from 25 ± 30 to 260 ± 30$^{14}$C yr, with regional weighed means ranging from 52 ± 47 to 196 ± 128 $^{14}$C yr (Figure 3). Anomalous $^{14}$C dates can be observed in five samples (shown in bold in Table 1), and were not considered for the calculation of the regional mean. Three were discarded because of ancient $^{14}$C dates (Arica 1948, Niebla 1911 and Niebla 1960 AD), one was not used for mean ΔR calculations due to potential $^{14}$C artifacts in the gastropod species *Littorina peruviana* (Valparaíso 1953), and one sample from Hoste Island (1954) was not used because of the clear influence of bomb-derived $^{14}$C (negative $^{14}$C ages). ANOVA statistical analysis of the set of mean ΔR ages from the Chilean coast reveal significant differences between all regions ($p < 0.001$), with the exception of the northern ΔR value against 33°S mean which have no significant differences. Nevertheless, there is a clear latitudinal tendency of decreasing values along the coast exists as shown in Figure 2.

### Marine Species Habitat and Feeding Mode

Selection of mollusks species for calculating ΔR values is important because the source of the carbon from which their shells is formed can be derived from dissolved inorganic carbon (DIC) of the seawater as well as carbon derived from metabolic processes like feeding in different proportions (Tanaka et al. 1986; Lorrain et al. 2004; McConnaughey and Gillikin 2008). In fact, Gillikin et al. (2006) showed that metabolic carbon varies from 10 to 35% in mollusks shells. Because of this, it is important to know the feeding habits and the environment where selected specimens lived. Ideally, chosen species for $^{14}$C dating should preferably be those with suspension-feeding habits, like bivalves, because they incorporate phytoplankton at the same time they absorb DIC (Tanaka et al. 1986; Forman and Polyak 1997) and are considered to be in equilibrium with seawater DIC (Hogg et al. 1998).

In contrast, gastropods may incorporate aged carbon from other sources like limestone, thus incorporating another unknown reservoir effect becoming unreliable for ΔR calculations (Dye 1994). Pigati et al. (2010) performed a comprehensive analysis of the presence of "dead carbon" in small terrestrial gastropods of 3749 individual shells to test the reliability of $^{14}$C dating in these organisms. They found a nearly 78% of the samples without influence of the limestone problem, bringing reliable $^{14}$C dates even when the shells where collected at sites with strong influence of carbonate rocks. More recently, Macario et al. (2016) did not find significant differences in $^{14}$C ages of terrestrial gastropods in the Brazilian coast. They analyzed the $^{14}$C content of individuals of the genera *Megalobulimus* and *Thaumastus* from the bomb-period (1948–2004). They found that the samples were not affected by the presence of limestone albeit their habitat was strongly influenced by carbonate rocks, and represented consistently the atmospheric $^{14}$C concentration during the time they lived. Despite Pigati et al. (2010) and Macario et al. (2016) results seem encouraging for the inclusion of gastropods in $^{14}$C reservoir assessments, we consider that further analysis is needed in marine organisms before including these organisms in $^{14}$C age studies. Although there is no sufficient information to extrapolate this to the marine environment, this may be used as an indicator of the confidence of dating gastropods shells. Along the coast of Chile, there are marine sedimentary rocks distributed

https://doi.org/10.1017/RDC.2018.81 Published online by Cambridge University Press

intermittently from the north down to around Chiloé (42°S, Paskoff 2010) which might contribute to the addition of ancient carbon to the coastal mollusk shells if they are truly using it. According to the SERNAGEOMIN (Chilean Geology and Mining Service) Chilean Geologic map, two of our sample sites might present carbonate rocks: Antofagasta (23°S), which is located over a Pleistocene coastal marine sedimentary sequence of biogenic carbonates, and the Magallanes Strait (53°S), which presents a complex geological formation dominated by deposits of glacial and fluvial origin as well as Mesozoic-Cenozoic granite batholiths (Hervé et al. 2009) but also has Cretaceous and Paleogene marine sedimentary sequences. In these locations, our data do not show any anomalously large ΔR estimates with the exception of Puerto Natales (see below).

The species used in this study were selected under the criteria of calendar year, favoring pre-bomb samples. In order to complete ΔR gaps along the Chilean coast, we chose to include samples that could present problems due to deposit feeding habits. Other studies have been performed dating deposit feeder shellfishes and carnivorous gastropods (Hogg et al. 1998; Soares and Dias 2006), and apparently there are no important differences attributable to the feeding way of the organisms, but results obtained from this mollusk type need to be analyzed with caution. At 33°S for example, ΔR values were exclusively obtained from deposit-feeders. This is not ideal since gastropods can scrape and take dead carbon from their feeding substrate. Notwithstanding, our results match the ΔR values obtained by Taylor and Berger (1967) and Ingram and Southon (1996) for the same locality and there is no indication of large amount of dead carbon influencing our ΔR estimations. We excluded a *Littorina peruviana* ΔR estimation from the regional mean because of some enriched $^{14}C$ giving a negative ΔR value as is the case with the periwinkle *Littorina littorea* (Petchey et al. 2012). Freshwater input through rivers or runoff can bring $CO_2$ derived from organic debris product of plants or soil decomposition, which can result in lower reservoir ages (Stuiver and Braziunas 1993; Southon et al. 2002). This result suggests that ΔR variability observed at 33°S, is to a great extent influenced by environmental variability like seasonal upwelling regimes or freshwater detritus-carbon input, whereas more southern reservoir ages are governed by low salinity and low temperature waters that favor $CO_2$ exchange between the surface ocean and the atmosphere.

### ΔR and Regional Oceanography

According to Toggweiler et al. (1991), ESSW upwells in the Peru and northern Chilean coastal region with the lowest $\Delta^{14}C$ signal across the Pacific. We infer that this is causing the higher ΔR values found in the northern part of our study region down to 40°S as shown by our data. Permanent upwelling regimes off northern Chile (20–30°S) promote higher ΔR ages than those found in the south, where this process presents seasonal intermittency (Letelier et al. 2009). We attribute the large variability in ΔR values observed at mid-latitude coastal localities like Valparaíso (33°S, Figure 2) to this intermittency. New ΔR data calculated for this region (n = 4) ranges from a minimum of 80 ± 38 to a maximum of 260 ± 30 $^{14}C$ yr bracketing well previous values published by Taylor and Berger (1967), Ingram and Southon (1996) and Carré et al. (2016). When analyzed together, all the data for this region give a mean ΔR of 148 $^{14}C$ yr with a large standard deviation of ± 78$^{14}C$ yr. At the open ocean site of the Juan Fernández archipelago (between 78.5° and 80.5°W, ca. 800 km from the Chilean coast) a low ΔR of 40 ± 38 $^{14}C$ yr compares well with the extensive dataset of Petchey et al. (2008) for the south Pacific Subtropical Gyre island system. We note that this is the first time that a ΔR value is given for this area.

The data for the central-south region of this study comprise the localities of Penco, San Vicente and Quiriquina Island (located inside the Bay of Concepción all located near 37°S, and showing

https://doi.org/10.1017/RDC.2018.81 Published online by Cambridge University Press

a ΔR mean of 194 ± 24 $^{14}$C yr. This zone is characterized by strong seasonal upwelling of $^{14}$C-depleted subsurface waters like off Valparaíso, although in this case, the data clusters well around the mean (low standard deviation). These values are the first published for this region.

Further south around 42°S, ΔR ages decrease to a mean of 141 ± 43 $^{14}$C yr, ranging from 55 ± 38 to 215 ± 38 $^{14}$C yr. Although climatologically this latitude south of the main northerly upwelling-favorable wind region, strong seasonal variability might include upwelling events (Letelier et al. 2009). The species analyzed from this region are mostly bivalves, with two exceptions (*Crepidula* sp. and *Purpura xanthostoma*), which are in good agreement with respect to their ΔR (170 ± 34 and 180 ± 34 $^{14}$C yr, respectively) with the rest of the data. The variability observed is probably related to different water mass influences as suggested by the carbonate $\delta^{13}$C data. Broadly, this region is bathed by SAAW, probably advecting a surficial $^{14}$C-depleted signal originated at the Southern Ocean upwelling region. SAAW presents high $\delta^{13}$C values (>1‰, Kroopnick 1985) due to high productivity and $CO_2$ consumption by phytoplankton. Primary productivity estimates in this region can reach values between 1 and 23 mg C m$^{-3}$ hr$^{-1}$ in winter and spring seasons, respectively (Iriarte et al. 2007). Besides, episodes of upwelling of subsurface waters can be present at this latitude and may decrease the $^{13}$C isotopic signal because of organic matter remineralization at deeper waters. According to Silva and Neshyba (1979), ESSW can reach latitudes as far as 45°S and it is possible that it brings its lower $\delta^{13}$C signal (<1‰) to the surface. Those water masses isotopic signals may be affecting the $^{13}$C content that is being taken by coastal mollusk to build their shells. However, there is also a large input of fresh water by precipitation, which might contribute to a reduction of the reservoir effect (Stuiver and Braziunas 1993; Southon et al. 2002) of this region and to the south, as well as large tidal cycles that could encourage gaseous mixing between the surface ocean and the atmosphere (Ingram and Southon 1996). In summary, we expect a large ΔR variability at this part of the ocean on seasonal and interannual time-scales, as shown by the data.

Southward, between 51° and 54°S, we have calculated eight new ΔR values ranging from 25 ± 30 to 60 ± 30 $^{14}$C yr. These values are significantly lower thanthe one reported by Ingram and Southon (1996) of 220 ± 46 $^{14}$C yr for Puerto Natales (51°S). We note that our new data comes from open to relatively open water locations and therefore, the large difference might be the result of complex oceanographic processes acting upon ΔR and by the large difference between water-mass ΔR endmembers in this area. For instance, SAAW can occasionally mix with fjord waters (Silva et al. 2009) lowering the$^{14}$C concentration (increasing ΔR) inland. In addition, Puerto Natales is located at the Señoret Fjord which is far from the open ocean and adjacent to the large Montt gulf. There are indications that strong hypoxia develops at the bottom of the Montt gulf, which could imply that below the sill depth, waters could age considerably potentially influencing surface ΔR values (Robert B. Dunbar, pers. comm.). Besides, lower values of ΔR are expected from the uptake of atmospheric $CO_2$ resulting from a greater solubility in seawater due to a lower temperature and salinity, $CO_2$ subsaturation of surface waters and the lack of coastal upwelled-waters (Siani et al. 2000; Torres et al. 2011). Therefore, we believe that these factors must be taken into account when choosing a ΔR value for marine $^{14}$C calibrations in materials from this area.

Based on our new and previously published data we therefore suggest five broad regional mean ΔR values based on predominant oceanographic processes occurring along the Chilean coast. These are: Northern upwelling system (18–30°S), Central upwelling system (30–33°S), Southern upwelling system (33–39°S), Northern Patagonia (39–43°S) and Southern Patagonia (43–55°S) (Figure 3).

https://doi.org/10.1017/RDC.2018.81 Published online by Cambridge University Press

### ΔR and $pCO_2$

$CO_2$ content of surface waters along the Chilean coast from 18° to about 40°S is intimately related to the upwelling of $CO_2$-saturated subsurface waters (Latorre et al. 2017). In fact, ΔR values along the coast fit well with the mean $\Delta pCO_2$ (the difference in the ocean-atmosphere $CO_2$ partial pressures, calculated such that positive values represent a larger ocean *p*CO2 and therefore a $CO_2$ efflux to the atmosphere) data of Torres et al. (2011).

From 40–42°S toward the pole, the combination of reduced upwelling, enhanced local biological productivity, the strengthening of wind stress at the surface and a greater solubility of $CO_2$ in colder seawater, promotes major $CO_2$ uptake into the ocean from the atmosphere, renewing its surface $^{14}C$ content and thus, diminishing ΔR values of the surface (Siani et al. 2000). In fact, wind speed has an important influence on gas transfer between the atmosphere and the ocean (Takahashi 2001), because increasing of atmospheric transfer of $CO_2$ to the ocean is directly related to higher wind speeds close to the surface. Along the Chilean coast, a trend of poleward increasing wind speed values has been reported according to Takahashi et al. (2002) and Torres et al. (2011), ranging from 5.5 m/s at 19°S to 11 m/s at 54°S, with maximum reported values >20 m/s. In addition, this increase in speed is also related to a change of direction from upwelling favorable southerly winds inthe region between 18° to 40–42ºS to a net westerly direction south of it. In fact, Bard (1988) and Bard et al. (1994) reported that changes in mean wind speed of 50% can result in 100 $^{14}C$ yr lower ΔR values.

## CONCLUSIONS

$^{14}C$ measurements on museum shells of known age were used to calculate new ΔR estimates for the Chilean coast, filling an important latitudinal gap from 33 to 53°S. In general, our estimates for the upwelling region north of 42ºS are in good agreement with previously published data. For this region ΔR weighed mean values range from $141 \pm 43$ to $196 \pm 128$ $^{14}C$ yr, thus we recommend using $180 \pm 27$ $^{14}C$ yr as a reasonable choice for the calibration of marine material from the upwelling favorable wind section of the Chilean coast. For the southern Patagonian Fjord area we calculated a mean of $52 \pm 47$ $^{14}C$ yr at 53ºS. These lower values represent the combined effect of reduced SST and sea surface salinity affecting the $\Delta pCO_2$ between the ocean and the atmosphere, with higher $\Delta pCO_2$ values being associated with higher ΔR (older waters). Finally, for the open ocean setting of the Juan Fernández archipelago, our data show a relatively minor i.e. $40 \pm 38$ $^{14}C$ yr deviation from the global modern ocean-atmosphere difference of 400 yr. We believe these that these results will improve considerably our knowledge of the modern ΔR corrections needed for reliable calibration of $^{14}C$ measurements of marine-derived materials for the Chilean coast.

## ACKNOWLEDGMENTS

We thank the curator of the Museum of Zoology of the University of Concepción, Dr. Jorge Artigas, and the personnel of the Chilean National Museum of Natural History: curator Andrea Martínez, Dr. Sergio Letelier and Dr. Oscar Gálvez for the help provided with the samples. Funding was provided by FONDAP 15110009, Iniciativa Científica Milenio NC120066 and FONDECYT Grants #1140536 (RDP-H), #11100281 (RDP-H) and #1150763 (CL, RDP-H). We finally thank associate editor Quan Hua, Matthew Carré, and an anonymous reviewer for their helpful comments, which improved the quality of this manuscript considerably.

## REFERENCES


Acha EM, Mianzan HW, Guerrero RA, Favero M, Bava J. 2004. Marine fronts at the continental shelves of austral South America, physical and ecological processes. *Journal Marine Systems* 44:83–105.

Alves EQ, Macario K, Ascough P, Bronk Ramsey C. 2018. The worldwide marine radiocarbon reservoir effect: Definitions, mechanisms, and prospects. *Reviews of Geophysics* 56: 278–305.

Ascough PL, Cook GT, Dugmore AJ. 2005. Methodological approaches to determining the marine radiocarbon reservoir effect. *Progress in Physical Geography* 29:532–47.

Bard E. 1988. Correction of accelerator mass spectrometry $^{14}C$ ages measured in planktonic foraminifera: paleoceanographic implications. *Paleoceanography* 3: 635–45.

Bard E, Arnold M, Mangeru J, Paterne M, Labeyrie L, Duprat J, Mélières M, Sonstegaard E, Duplessy J. 1994. The North Atlantic atmosphere-sea surface $^{14}C$ gradient during the Younger Dryas climatic event. *Earth and Planetary Science Letters* 126:275–87.

Berkman PA, Forman SL. 1996. Pre-bomb and the reservoir correction for calcareous marine species in the Southern Ocean. *Geophysical Research Letters* 23(4):363–6.

Broecker WS. 1987. The great ocean conveyor. *Natural History Magazine* 97:74–82.

Broecker WS, Klas M, Clark E, Bonani G, Ivy S, Wolfli W. 1991. The influence of $CaCO_3$ dissolution on core top radiocarbon ages for deep sea sediments. *Paleoceanography* 6(5):593–608.

Carré M, Jackson D, Maldonado A, Chase B, Sachs P. 2016. Variability of $^{14}C$ reservoir age and air-sea flux of $CO_2$ in the Perú-Chile upwelling region during the past 12,000 years. *Quaternary Research* 85:87–93.

Cook GT, MacKenzie AB, Muir GKP, Mackie G, Gulliver P. 2004. Sellafiel-derived anthropogenic $^{14}C$ in the marine intertidal environment of the NE Irish Sea. *Radiocarbon* 46(2):877–83.

Culleton BJ, Kennett DJ, Ingram BL, Erlandson JM, Southon JR. 2006. Intrashell radiocarbon variability in marine mollusks. *Radiocarbon* 48(3): 387–400.

Dávila P, Figueroa D, Müller E. 2002. Freshwater input into the coastal ocean and its relation with the salinity distribution off austral Chile (35–55°S). *Continental Shelf Research* 22:521–34.

Druffel E. 1981. Radiocarbon in annual coral rings from the eastern tropical Pacific Ocean. *Geophysical Research Letters* 8(1):59–62.

Druffel E, Griffin S. 1995. Regional variability of surface ocean radiocarbon from southern Great Barrier Reef corals. *Radiocarbon* 37(2): 517–24.

Dye T. 1994. Apparent ages of marine shells: Implications for archaeological dating in Hawaii. *Radiocarbon* 36(1):51–7.

Forman S, Polyak L. 1997. Radiocarbon content of pre-bomb marine mollusks and variations in the $^{14}C$ reservoir age for coastal areas of the Barents and Karaseas, Russia. *Geophysical Research Letters* 24(8):885–8.

Gillikin D, Lorrain A, Bouillon S, Willenz P, Dehairs F. 2006. Shell carbon isotopic composition of Mytilusedulis shells: relation to metabolism, salinity, $\delta^{13}C$ DIC and phytoplankton. *Organic Geochemistry* 37:1371–82.

Goodfriend GA, Flessa KW. 1997. Radiocarbon reservoir ages in the Gulf of California: Roles of upwelling and flow from the Colorado River. *Radiocarbon* 39(2):139–48.

Guilderson T, Schrag D, Goddard E, Kashgarian M, Wellington G, Linsley B. 2000. Southwest Subtropical Pacific surface water radiocarbon in a high-resolution coral record. *Radiocarbon* 42(2): 249–56.

Heier-Nielsen S, Heinemeier J, Nielsen HL, Rud N. 1995. Recent reservoir ages for Danish fjords and marine waters. *Radiocarbon* 37(3):875–82.

Hervé F, Quiroz D, Duhart P. 2009. Main geological aspects of the Chilean Fjord Region. In: Vreni Hausserman V, Försterra G, editors. *Marine Benthic Fauna of Chilean Patagonia*. Santiago: Nature in Focus. p 30–42.

Hinojosa J, Moy C, Prior C, Eglinton T, McIntyre C, Stirling C, Wilson G. 2015. Investigating the influence of regional climate and oceanography on marine radiocarbon reservoir ages in southwest New Zealand. *Estuarine, Costal and Shelf Science* 167:526–39.

Hogg A, Higham T, Dahm J. 1998. $^{14}C$ dating of modern marine and estuarine shellfish. *Radiocarbon* 40(2):975–84.

Hua Q. 2009. Radiocarbon: A chronological tool for the recent past. *Quaternary Geochronology* 4: 378–90.

Hughen KA, Baillie MGL, Bard E, Beck JW, Bertrand CJH, Blackwell PG, Buck CE, Burr GS, Cutler KB, Damon PE, Edward RL, Fairbanks RG, Friedrich M, Guilderson TP, Kromer B, McCormac G, Manning S, Bronk Ramsey C, Reimer PJ, Reimer RW, Remmele S, Southon JR, Stuiver M, Talamo S, Taylor FW, van der Plicht J, Weyenmeyer CE. 2004. Marine04 marine radiocarbon age calibration, 0–26 cal kyr BP. *Radiocarbon* 46(3):1059–86.

Ingram B, Southon J. 1996. Reservoir ages in eastern Pacific coastal and estuarine waters. *Radiocarbon* 38(3):573–82.

Iriarte JL, González HE, Liu KK, Rivas C, Valenzuela C. 2007. Spatial and temporal variability of chlorophyll and primary productivity in surface


https://doi.org/10.1017/RDC.2018.81 Published online by Cambridge University Press

waters of southern Chile (41.5-43°S). *Estuarine, Coastal and Shelf Science* 74:471–80.

Kroopnick PM. 1985. The distribution of $^{13}C$ of $\sum CO_2$ in the world oceans. *Deep-Sea Research* 32(1):57–84.

Latorre C, De Pol-Holz R, Carter C, Santoro C. 2017. Using archaeological Shell middens as a proxy for past local coastal upwelling in northern Chile. *Quaternary International* 427A: 128–36.

Letelier J, Pizarro O, Nuñez S. 2009. Seasonal variability of coastal upwelling and the upwelling front off central Chile. *Journal of Geophysical Research* 114: C12009.

Lorrain A, Paulet Y, Chauvaud L, Dunbar R, Mucciarone D, Fontugne M. 2004. $\delta^{13}C$ variation scallop shells: increasing metabolic carbon contribution with body size?. *Geochimica et Cosmochimica Acta* 68(17):3509–19.

Loyd D, Vogel J, Trumbore S. 1991. Lithium contamination in AMS measurements of $^{14}C$. *Radiocarbon* 33(3):297–301.

Macario KD, Alves EQ, Carvalho C, Oliveira FM, Bronk Ramsey C, Chivall D, Souza R, Simone LRL, Cavallari DC. 2016. The use of the terrestrial snails of the genera *Megalobulimus* and *Thaumastus* as representatives of the atmospheric carbon reservoir. *Scientific Reports* 6:27395. doi: 10.1038/srep27395.

Mc Connaughey T, Gillikin D. 2008. Carbon isotopes in mollusk shell carbonates. *Geo-Marine Letters* 28:287–99.

Ortlieb L, Vargas G, Saliège JF. 2011. Marine radiocarbon reservoir effect along the northern Chile–southern Peru coast (14–24°S) throughout the Holocene. *Quaternary Research* 75:91–103.

Paskoff R. 2010. Geomorfología de la costa de Chile. En: Geología marina. *Comité Oceanográfico Nacional. Chile*. p. 76–83.

Petchey F, Anderson A, Zondervan A, Ulm S, Hogg A. 2008. New marine ΔR values for the south Pacific Subtropical Gyre region. *Radiocarbon* 50(3): 373–97.

Petchey F, Ulm S, David B, McNiven I, Asmussen B, Tomkins H, Richards T, Rowe C, Leavesley M, Mandui H, Stanisic J. 2012. $^{14}C$ Marine reservoir variability in herbivores and deposit–feeding gastropods from an open coastline, Papua New Guinea. *Radiocarbon* 54(3–4):967–78.

Pigati J, Rech J, Nekola J. 2010. Radiocarbon dating of small terrestrial gastropod shells in North America. *Quaternary Geochronology* 5:519–32.

Reimer O, Bard E, Bayliss A, Beck J, Blackwell P, Bronk C, Buck C, Cheng H, Lawrence R, Friedrich M, Grootes P, Guilderson T, Haflidason H, Hajdas I, Hatté C, Heaton T, Hoffman D, Hogg A, Hughen A, Kaiser K, Kromer B, Manning S, Niu M, Reimer R, Richards D, Scott E, Southon J, Staff R, Turney C, van der Plicht J. 2013. IntCal13 and Marine13 radiocarbon age calibration curves 0–50,000 years Cal BP. *Radiocarbon* 55(4):1869–87.

Shaffer G, Hormazábal S, Pizarro O, Salinas S. 1999. Seasonal and interannual variability of currents and temperature off central Chile. *Journal of Geophysical Research* 104:29951–61.

Siani G, Paterne M, Arnold, Bard E, Métivier B, Tisnerat N, Bassinot F. 2000. Radiocarbon reservoir ages in the Mediterranean Sea and Black sea. *Radiocarbon* 42(2):271–80.

Silva N, Calvete C, Sievers H. 1997. Características oceanográficas físicas y químicas de canales australes chilenos entre Puerto Montt y laguna San Rafael (Crucero Cimar Fiordo1). *Ciencia y Tecnología del Mar* 20:23–106.

Silva N, Neshyba S. 1977. Corrientes superficiales frente a la costa austral de Chile. *Ciencia y Tecnología del Mar* 3:37–42.

Silva N, Neshyba S. 1979. On the southernmost extension of the Perú–Chile Undercurrent. *Deep–Sea Research* 26:1387–93.

Silva N, Rojas N, Fedele A. 2009. Water masses in the Humboldt Current System: Properties, distribution, and the nitrate deficit as a chemical water mass tracer for Equatorial subsurface water off Chile. *Deep-Sea Research II* 56:1004–20.

Silva N, Vargas C. 2014. Hypoxia in Chilean Patagonian Fjords. *Progress in Oceanography* 129A:62–74.

Soares A, Dias J. 2006. Coastal upwelling and radiocarbon – evidence for temporal fluctuations in ocean reservoir effect off Portugal during the Holocene. *Radiocarbon* 48(1):45–60.

Southon J, Kashgarian M, Metivier B, Yim WS 2002. Marine reservoir corrections for the Indian Ocean and Southeast Asia. *Radiocarbon* 44(1): 167–80.

Southon J, Oakland A, True D. 1995. A comparison of marine and terrestrial radiocarbon ages from Northern Chile. *Radiocarbon* 37(2):389–93.

Strub T, Mesías J, Montecino V, Rutllant J, Salinas S. 1998, Coastal ocean circulation off western South America. In: Robinson AR, Brink KH, editors. *The Sea*. p. 273–313.

Stuiver M, Braziunas T. 1993. Modeling atmospheric $^{14}C$ influences and $^{14}C$ ages of marine samples back to 10,000 B.C. *Radiocarbon* 35(1):137–91.

Stuiver M, Pearson G, Braziunas T. 1986. Radiocarbon age calibration of marine samples back to 9,000 cal yr BP. *Radiocarbon* 28(2B):980–1021.

Stuiver M, Polach H. 1977. A discussion and reporting of $^{14}C$ data. *Radiocarbon* 19(3):355–63.

Takahashi T. 2001. *Carbon Dioxide ($CO_2$) Cycle*. Columbia University: Academic Press. p. 400–7.

Takahashi T, Sutherland S, Sweeney C, Poisson A, Metzl N, Tilbrook B, Bates N, Wannikhof R, Feely R, Sabine C, Olafsson J, Nojiri Y. 2002. Global sea–air $CO_2$ flux based on climatological surface ocean $pCO_2$, and seasonal biological and temperature effects. *Deep Sea Research II* 49:1601–22.

Tanaka N, Monaghan MC, Rye DM. 1986. Contribution of metabolic carbon to mollusk and barnacle shell carbonate. *Nature* 320:520–3.

https://doi.org/10.1017/RDC.2018.81 Published online by Cambridge University Press

Taylor R, Berger R. 1967. Radiocarbon content of marine shells from the Pacific coast of central and South America. *Science.* 158:1180–2.

Toggweiler J, Dixon K, Broecker W. 1991. The Peru upwelling and the ventilation of the South Pacific Thermocline. *Journal of Geophysical Research* 96 (11):20467–97.

Torres R, Pantoja S, Harada N, González H, Daneri G, Frangopulos M, Rutlant J, Duarte C, Rúiz-Halpern S, Mayol E, Fukasawa M. 2011. Air-sea $CO_2$ fluxes along the coast of Chile: From $CO_2$ outgassing in central northern upwelling waters to $CO_2$ uptake in southern Patagonian fjords. *Journal of Geophysical Research* 116. C09006.

Vogel J, Southon J, Nelson D, Brown T. 1984. Performance of catalytically condensed carbon for use in accelerator mass spectrometry. In: Wolfli W, Polach H, Andersen H, editors. Proceedings, 3rd International Conference on AMS. *Nuclear Instruments and Methods* B5: 289.

Wanninkhof R, McGillis WR. 1999. A cubic relationship between air-sea $CO_2$ exchange and wind speed. *Geophysical Research Letters* 26 (13):1889–92.

https://doi.org/10.1017/RDC.2018.81 Published online by Cambridge University Press